

## Demonstration of numerical simulation of multi-dimensional two-phase flow for a marine reactor

Myung-Ho Kim<sup>a</sup>, Byoung-Jae Kim<sup>a\*</sup>

<sup>a</sup>Department of Mechanical Engineering, Chungnam National University, 99 Daehak-ro, Yuseong-gu, Daejeon 34134

\*Corresponding author: bjkim@cnu.ac.kr

### 1. Introduction

Recently, a marine reactor received a great attention in Korea [1-2]. The marine reactor can secure safety from natural disasters like tsunami. The floating marine nuclear power supplies power to the surrounding facilities from the coast or ocean [2]. It is a way to develop resources in the ocean.

A floating ship may show an unexpected behavior in response to external conditions such as ocean waves and currents. In this case, one must consider the effect of the ship motion on the thermo-fluid dynamics in the reactor.

There are two choices to predict a flow behavior in the moving body. One is to apply the existing two-fluid equations to a two-phase flow in a moving body in the absolute frame of reference. The other is to use the proper two-fluid equations in the non-inertial frame of reference. The latter is preferred because the moving body can be fixed in the simulation domain.

Kim et al. (2017) proposed the multi-dimensional two-fluid equations in the non-inertial coordinates [3]. This paper demonstrates the numerical simulations using the proposed equations.

### 2. Numerical Methods

#### 2.1 Governing equations

According to Kim et al. (2017), for an adiabatic two-phase flow, the two-fluid momentum equation in the non-inertial coordinates is given by

$$\frac{\partial}{\partial t}(\alpha_k \rho_k \mathbf{u}_k) + \nabla \cdot (\alpha_k \rho_k \mathbf{u}_k \mathbf{u}_k) = -\alpha_k \nabla p + \nabla \cdot [\alpha_k (\boldsymbol{\tau}_k + \boldsymbol{\tau}_k^{Re})] + \alpha_k \rho_k \mathbf{g} + \mathbf{M}_{ik} + \mathbf{F}_{fictitious} \quad (1)$$

This equation is the same as the existing equation, except for the last term. The fictitious force term is

$$\mathbf{F}_{fictitious} = -\alpha_k \rho_k \ddot{\mathbf{R}} - \alpha_k \rho_k \dot{\boldsymbol{\Omega}} \times \mathbf{r}_k - 2\alpha_k \rho_k \boldsymbol{\Omega} \times \mathbf{u}_k - \alpha_k \rho_k \boldsymbol{\Omega} \times (\boldsymbol{\Omega} \times \mathbf{r}_k) \quad (2)$$

where  $\ddot{\mathbf{R}}$  represent the linear acceleration of the moving frame relative to the absolute frame,  $\dot{\boldsymbol{\Omega}}$  is the rotation vector of the moving frame relative to the absolute frame, and  $\mathbf{r}_k$  is the local position vector relative to the rotation origin in the moving frame.

#### 2.2 Two-phase models

In Eq. (1),  $\mathbf{M}_{ik}$  stands for the interfacial momentum transfer. One can write

$$\mathbf{M}_{ik} = \mathbf{f}_D + \mathbf{f}_L + \mathbf{f}_{wL} + \mathbf{f}_{TD} + \mathbf{f}_{VM} \quad (3)$$

where  $\mathbf{f}_D$ ,  $\mathbf{f}_L$ ,  $\mathbf{f}_{wL}$ ,  $\mathbf{f}_{TD}$ , and  $\mathbf{f}_{VM}$  are the interfacial drag, lift, wall lubrication, turbulent dispersion, and virtual mass, respectively.

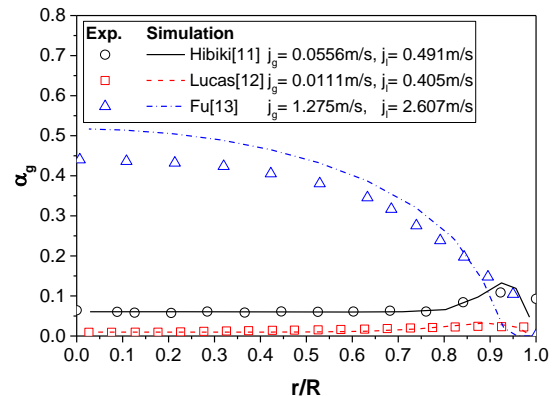
In this study, Grace's model [4] was used for the interfacial drag. This model is recommended for large deformable bubbles. Tomiyama's model [5] was used for the lift force. The main advantage of this model is that the value of the lift coefficient depends on the bubble diameter. Antal's model [6] was used for the wall lubrication force. [7] suggested  $C_{w,1} = -0.055$  and  $C_{w,2} = 0.09$ , and we adopted these values for Antal's model. Burns' model [8] was used for the turbulent dispersion force. As for the liquid turbulence, we used the K- $\omega$  SST model [9]. In addition, Sato's model [10] was used to consider the bubble-induced turbulence.

### 3. Simulation in stationary channels

Figure 1 compares the numerical simulation results with the experimental data for stationary circular pipes. Detailed experimental conditions can be found in the corresponding references.

The void fraction profiles are plotted across the pipe. One can see that not only the wall-peaking profile but also the core-peaking profile is well predicted.

We also performed numerical simulations in a rectangular channel (0.1 × 0.02 × 1.0 m) [15]. Initially, the channel is filled with water. The air is injected from



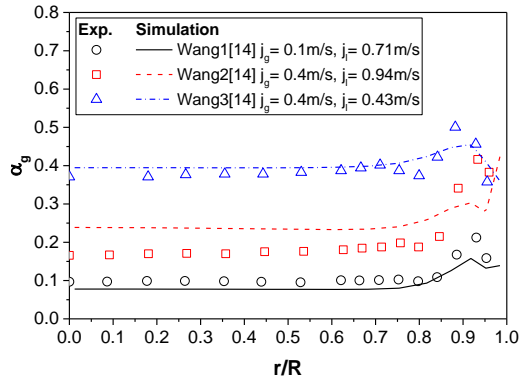


Fig. 1. Void fractions across the stationary circular pipes

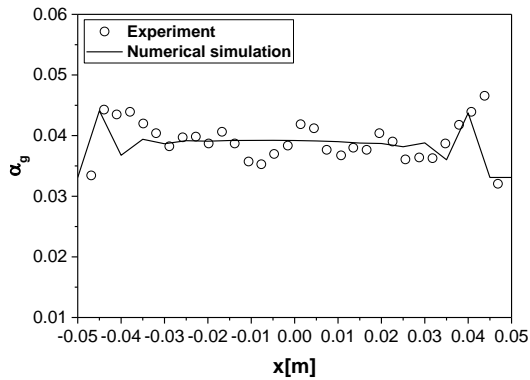


Fig. 2. Time-averaged void fractions at a height of 0.63 m in the stationary rectangular channel.

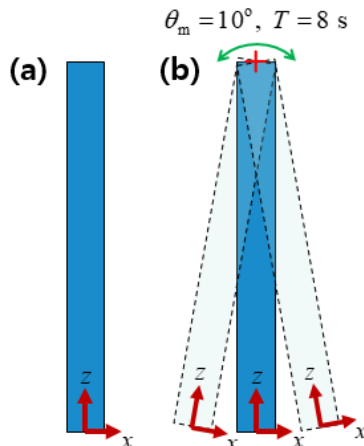


Fig. 3 Krepper's rectangular channel. a) stationary, b) oscillating ( $\theta_m = 10^\circ$  and  $T = 8$  s)

the inlet ( $0.02 \times 0.01$ m) placed at the bottom of the channel.

Although the volume flow rate of the air injection is constant in time, the flow oscillates. See [15] for the details.

Figure 2 shows the time-averaged void fractions at a height of  $z = 0.63$  m from the bottom ( $j_g = 10$  mm/s). The predicted void fractions show good agreement with the experimental void fractions.

From the results so far, one can tell that the present model set is acceptable for bubbly flow simulation.

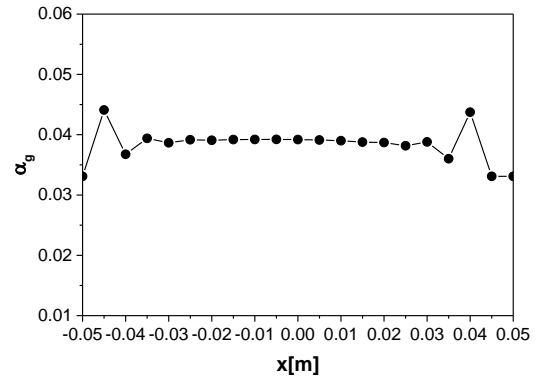


Fig. 4. Time-averaged void fraction profile for the stationary channel (numerical simulation)

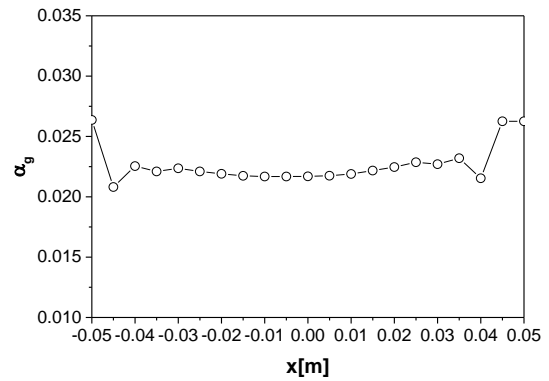


Fig. 5. Time-averaged void fraction profile for the oscillating channel (numerical simulation)

#### 4. Simulation in oscillating channels

Figure 3 delineates two cases of Krepper's rectangular channel. The left channel is the stationary case, whereas the right channel is oscillating ( $\theta = \theta_m \sin(2\pi t/T)$ ). Initially, the channel is filled with water. The air is injected through the whole bottom of the channel ( $u_g = 10$  mm/s)

Figure 4 shows the time averaged void fraction at a height of 0.63 m in the stationary channel. The void fraction is about 0.04 and nearly uniform across the channel. Figure 5 shows the result for the oscillating channel. It is interesting to note that the void fraction is considerably decreased compared to the stationary case. The oscillation leads to the significant decrease in the void fraction. This may be due to the centrifugal force caused by the rolling oscillation.

#### 5. Conclusions

Numerical simulations were carried out using the multi-dimensional two-fluid equations in the non-inertial frame of reference. It was shown that the rolling motion decreased the void fraction in the channel. Experiment will be performed to validate the simulation result.

#### Acknowledgement

This work was supported by the National Research Foundation of Korea(NRF) grant funded by the Ministry of Science, ICT & Future Planning (No. NRF-2016M2B2A9A02944972).

## REFERENCES

- [1] P. S. Lee, 국내외 해양원자력 시스템 개발현황 및 전망, 한국해양과학기술협의회 공동학술대회, 2014.
- [2] S. H. Han, K. W. Lee, 해양원자력시스템 사업화 방안, 해양-원자력 공동위원회, 2015.
- [3] B. J. Kim, J. H. Lee, J. Heo, and K. D. Kim\*, "Two-fluid equations for a two-phase flow system with arbitrary motions," submitted, 2017.
- [4] Grace, Clift and Weber. Bubbles, Drops, and Particles, Technical Report. Academic Press, 1978.
- [5] T. Takamasa, A. Tomiyama, Three-Dimensional Gas-Liquid Two-Phase Bubbly Flow in a C-Shaped Tube, Ninth International Topical Meeting on Nuclear Reactor Thermal Hydraulics (NURETH-9). San Francisco, CA., 1999.
- [6] Antal, S. P., Lahey, R. T., and Flaherty, J. E., Analysis of phase distribution in fully developed laminar bubbly two-phase flow, *Int. J. Multiphase Flow*, 7, pp. 635-652, 1991.
- [7] M. Colombo, M. Fairweather, Multiphase turbulence in bubbly flows: RANS simulations, *International Journal of Multiphase Flow*, Vol.77, pp. 222 - 243, 2015.
- [8] A. D. B. Burns, Th. Frank, I. Hamill, and J.-M. Shi. The Favre Averaged Drag Model for Turbulent Dispersion in Eulerian Multi-Phase Flows. Fifth International Conference on Multiphase Flow, ICMF-2004, Yokohama, Japan. 2004.
- [9] Bardina, J.E., Huang, P.G. and Coakley, T.J., Turbulence Modeling Validation Testing and Development, NASA Technical Memorandum 110446, 1997.
- [10] Sato, Y. and Sekoguchi, K., Liquid Velocity Distribution in Two-Phase Bubbly Flow, *Int. J. Multiphase Flow*, 2, p.79, 1975.
- [11] T. Hibiki, M. Ishii, Z. Xiao, Axial interfacial area transport of vertical bubbly flows, *Int. J. Heat Mass Transfer* 44(10) (2001) 1869-1888.
- [12] D. Lucas, E. Krepper, H. M. Prasser, Development of co-current air-water flow in a vertical pipe, *Int. J. Multiphase Flow* 31(12) (2005) 1304-1328.
- [13] X. Fu, Interfacial area measurement and transport modeling in air-water two-phase flow (PhD Thesis), Purdue University, 2001.
- [14] Q. Wang, W. Yao, Computation and validation of the interphase force models for bubbly flow, *International Journal of Heat and Mass Transfer*, Vol.98, pp. 799 - 813, 2016.
- [15] E. Krepper, H. M. Prasser, Measurements and CFX-Simulations of a bubbly flow in a vertical pipe, *Adv. Fluid Mech.* 26 (2000), 23-32.